





Research Article

Modeling of Concrete-Frozen Soil Interface from Direct Shear Test Results

Meng Xiong ^{1,2}, Pengfei He ^{1,2,3}, Yanhu Mu ^{2,3} and Xinlei Na ⁴

¹Lanzhou University of Technology, Lanzhou 730050, China

²State Key Laboratory of Frozen Soil Engineering, Northwest Institute of Eco-Environment and Resources, Chinese Academy of Sciences, Lanzhou 730000, China

³University of Chinese Academy of Science, Beijing 100049, China

⁴Geotechnical Group, Golder Associates Inc, Anchorage 99507, USA

Correspondence should be addressed to Yanhu Mu; muyanhu@lzb.ac.cn

Received 9 October 2019; Revised 17 December 2020; Accepted 19 December 2020; Published 4 January 2021

Academic Editor: Yinshan Tang

Copyright © 2021 Meng Xiong et al. This is an open access article distributed under the Creative Commons Attribution License, which permits unrestricted use, distribution, and reproduction in any medium, provided the original work is properly cited.

The shear behaviors of concrete-frozen soil interface are important for analyzing the performance of engineering structures buried in the frozen ground. In this paper, a series of direct shear tests were carried out to determine the concrete-soil interface behaviors at different test temperatures (19°C, -1°C, -3°C, and -5°C) and initial water contents (9.2%, 13.1%, 17.1%, and 20.8%) of soils. The interface shear behaviors, including the shear stress versus horizontal displacement, interface cohesion, and interface friction coefficient, were analyzed based on the test results. Then, a simple, nonlinear model was proposed and verified for the interface shear behaviors. The results show that the effect of initial water content and test temperature on the interface shear behavior is significant, and the peak stress increases with the increasing initial water content and decreasing test temperature. The interface cohesion is sensitive to the test temperature and initial water content, while the interface friction coefficient is insensitive to both the factors. The parameters of the simple nonlinear model can be gained by back-analyzing the test results. The predictions made by the proposed model are found to be in good agreement with the experimental results.

1. Introduction

The interface shear behaviors between concrete and frozen soil are significantly important for cold region engineering such as frost jacking of piles in seasonally frozen ground, stability of reinforced concrete gravity-retaining walls against sliding in seasonal soils, and concrete linings on compacted subgrade of canals to stop seepage losses. When the structures buried in the frozen soil are subjected to frost-heave force or external load, the relative slip and destruction between the frozen soil and structures will occur, in which the tangential force between the frozen soil and the structure interface is called the adfreeze force [1–3]. In the process of external loading, the adfreeze force is variable and the maximum is known as adfreeze strength [4, 5]. It is well-known that even a small displacement of a structure in frozen soil can destroy the adfreeze bond between soil and

structure [6]. Therefore, studies on the interface shear behavior or adfreeze strength of the frozen soil-structure are crucial for the engineering design and numerical simulation of the projects in cold regions.

The interface shear behaviors of the frozen soil-structure have been widely investigated using field tests [7–12], laboratory tests [3, 6, 13–17], and numerical simulations or theoretical analyses [18–21]. Liu et al. [14] investigated the shear behavior of frozen soil-concrete interface using a temperature-controlled direct shear test system, and their results showed that temperature and moisture content had a great effect on the peak shear strength but had little effect on the residual shear strength. Zhao et al. [22], Shi et al. [16], and Wang et al. [23] focused on the interface behavior of artificial frozen soil-steel interface commonly encountered during shield tunneling by Tunnel Boring Machine (TBM) and found that temperature and surface roughness had

significant influence on the interface shear behavior. Wen et al. [13] studied the adfreeze strength of frozen soil-fiberglass reinforced plastic interface by direct shear test in a temperature-controlled room and concluded that the cohesion was controlled by the temperature and moisture content, and the friction angle is, however, only affected by the moisture content. Ji et al. [24] tested the interface shear behavior between cast-in-situ concrete and frozen soil, and the results showed that the hydration heat of cement greatly affected the interface roughness and shear strength. These studies indicated that the adfreeze strength can be affected by the mechanical properties of soil and structural material, test temperature, initial water content, normal stress, and so on. In laboratory tests, the direct shear test is the most common method used for investigations on the interface shear behavior [25–28].

In order to simulate the interface behaviors, a series of elastic, plastic, linear, and nonlinear models were used. Duncan-Chang's hyperbolic model is the most common one to simulate the strain-hardening behavior of interface, but it is failing to simulate strain-softening behavior [29]. Some other models were also established, including the exponential function model [30, 31], power function model [32], damage constitutive model [33, 34], rigid-plastic model [35], fractal theory model [36], and DSC model [37]. These models can simulate different interface behaviors; however, they cannot simulate the strain-hardening and strain-softening behavior simultaneously, and there are generally too many parameters that are difficult to determine.

In this study, a series of direct shear tests for concrete-frozen soil interface were carried out at the different normal stresses, test temperatures, and initial soil water contents. The interface shear behaviors, including the shear stress versus horizontal displacement, interface cohesions, and friction coefficients were analyzed with the test results. Then, a nonlinear model was proposed to simulate the strain-softening and strain-hardening behaviors of concrete-frozen soil interface. The model parameters can be obtained for any specific problem by conducting such tests. Using these model parameters, the back-fitted shear stress versus horizontal displacement has been obtained and compared with the test results.

2. Experimental Method

2.1. Test Materials. Soil materials used in this study were taken from a shallow surface layer of Q4 loess in the Yongdeng County, China. First, the soil taken from the field was naturally dried, fully stirred, and crushed by a small test roller. Then, it was sifted with a 2 mm sieve. The index properties and grain size distribution of the tested soil specimens were obtained and are listed in Table 1 [38, 39]. The tested soils are classified as low liquid limit clay (CL) based on the unified soil classification system. After sieving, the tested soil was reconstituted by adding distilled water to a target initial water content by weight. Then, it was sealed for 12 hours to ensure that the initial water content was uniform [13].

Concrete specimens, 20 mm in height and 61.8 mm in diameter, were mixed using cement mortar, which was stirred from Ordinary Portland Cement (cement grade # PO 32.5) and natural river sand. The mix ratio of the cement, sand, and water was 1.8:3:1, respectively [40]. Larger particles such as gravel (>4.75 mm) were removed during this process due to the requirement for small sample size. All the specimens were cured for 28 days after pouring and forming according to the test method of long-term and durability on ordinary concrete [40]. The same batch of concrete was used in all tests in order to maintain a similar roughness and unified height.

The concrete-soil specimen was prepared as follows. First, the concrete specimen was placed at the bottom of a specimen cell which had a height of 40 mm and an inner diameter of 61.8 mm. Then, the tested soil was put into the cell above the concrete specimen and compacted to a target dry density of 1.68 g/cm^3 and a target height of 20 mm. Consequently, the concrete-soil specimen had a total height of 40 mm, and the concrete-soil interface was in the middle of the specimen and coincided with the shear plane of the shear box (Figures 1(a) and 1(b)). After that, the concrete-soil specimen was sealed with plastic film and refrigerated at a temperature of -20°C for 24 hours. The aim of quick-freezing the specimen was to prevent moisture migration in the soil. After quick-freezing, the concrete-soil specimen was placed in a constant temperature container for 12 hours to achieve a thermal balance. Figure 2 shows the temperature variations of the sample interface during quick-freezing, constant temperature processing, and the shearing test. It can be seen that the fluctuation of the temperature at interface during the shearing test is very slight, which illustrates a good precision of temperature control.

2.2. Test Procedures. The direct shear test of the concrete-soil interface was performed on a four-joint, strain-controlled direct shear apparatus made by Nanjing Soil Instrument Factory, Nanjing, China (Figure 1(c)). The shear apparatus consists of two shear boxes, namely, the lower box and the upper box, each of which has a height of 20 mm. The concrete-soil interface of the specimen overlapped with the shearing plane of the apparatus.

To investigate the effects of the initial water content of soils and the test temperature on the adfreeze strength of the concrete-soil interface, a series of direct shear tests with four initial water contents of 9.2%, 13.1%, 17.1%, and 20.8% and four test temperatures of 19°C , -1°C , -3°C , and -5°C were carried out in a temperature-controlled laboratory. The laboratory temperature was adjusted to be the same as the test temperature, with a precision of $\pm 0.5^\circ\text{C}$. The direct shear tests were performed with constant normal stresses of 50 kPa, 100 kPa, 200 kPa, and 300 kPa (as shown in Figure 1(d)). After applying the normal stress to the concrete-soil specimen, a constant shear displacement rate of 0.8 mm/min was applied to the lower box. A set of samples could be tested in 10 min; therefore, the fluctuation of temperature in the cold room had a slight influence on the inner temperature of the samples.

TABLE 1: Index properties and grain size distribution of the tested soil.

Liquid limit/%	Plastic limit/%	Specific gravity	Optimum water content/%	Grain size distribution/%			
				>0.25	0.05–0.25	0.005–0.05	<0.005
26.29	18.24	2.7	13.0	1.22	14.53	65.07	19.18

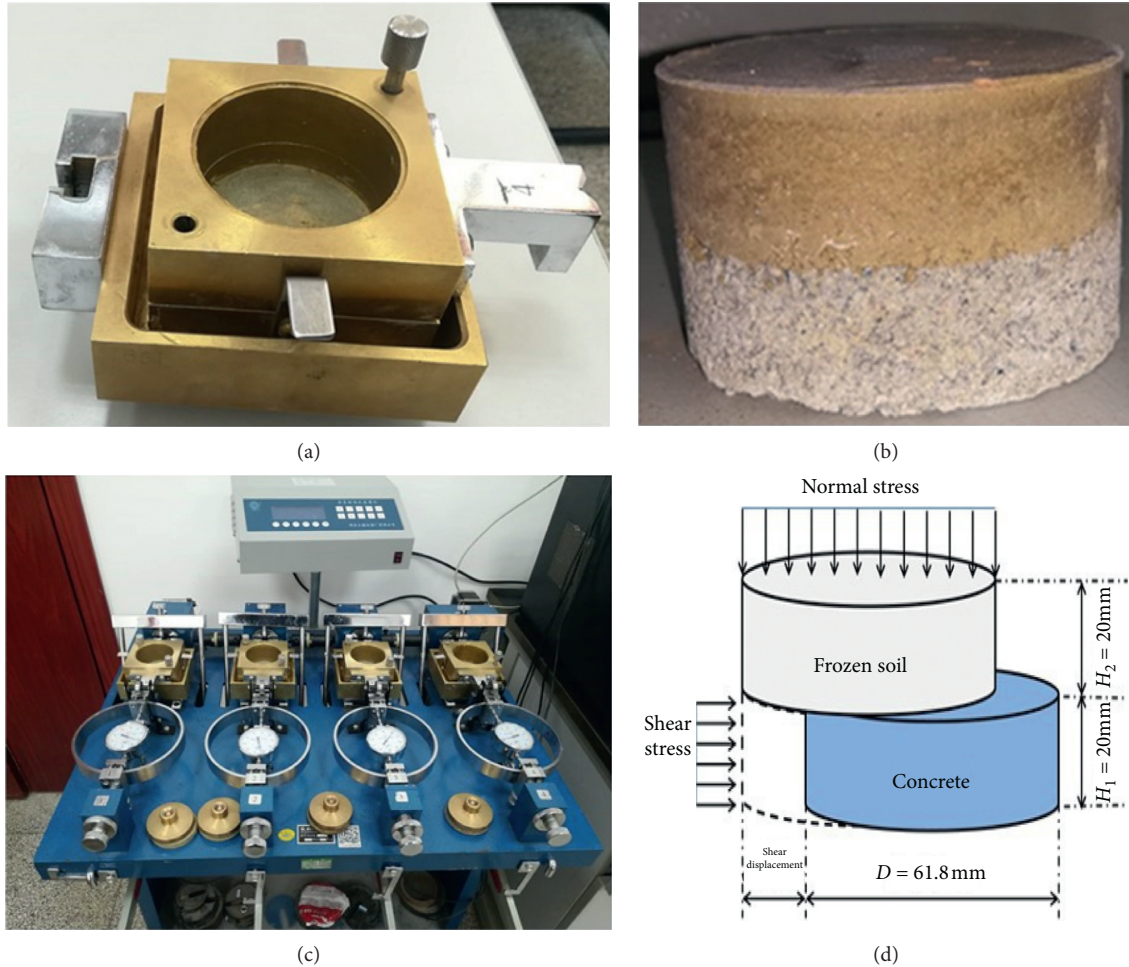


FIGURE 1: Test apparatus (a, c), the concrete-soil specimen (b), and stress state of the specimen during shearing (d).

2.3. Test Results. Figure 3 shows the shear stress versus horizontal displacement under different initial water contents and test temperatures at the normal stress of 100 kPa. The results at 19°C are shown in Figure 3(a); the concrete-soil interface exhibited a strain-softening behavior at the initial water content of 9.2% and 13.1%, while a strain-hardening behavior was exhibited at the initial water content of 17.1% and 20.8%. The initial tangent modulus is an important parameter for the interface shearing behaviors, and it can be calculated by the hyperbolic model. In Figure 4(a), it can be seen that the initial tangent modulus decreased obviously with the increasing initial water content. The peak shear stress decreased from 107.6 kPa to 60.6 kPa with an increase in the initial water content from 9.2% to 20.8%, likely due to decreasing matric suction resulting from increasing degree of saturation [41]. For the

tests at -1°C (Figure 3(b)), the concrete-frozen soil interface showed a strain-softening behavior at an initial water content of 9.2%, 13.1%, and 17.1%, while a strain-hardening behavior was evident at an initial water content of 20.8%. The initial tangent modulus decreased slightly with the increasing initial water content (Figure 4(b)). The peak shear stress decreased from 86.5 kPa to 70.7 kPa with the initial water content increasing from 9.2% to 20.8%. The test results at -3°C and -5°C are shown in Figures 3(c) and 3(d). It can be seen that the concrete-frozen soil interface demonstrated a predominant strain-softening behavior at all the four initial water contents. The shear stress increased quickly with increasing horizontal displacement initially, and a significant and rapid drop occurred after the shear stress reached its peak value. The initial tangent modulus decreased slightly with increasing initial water content at -3°C (Figure 4(c)),

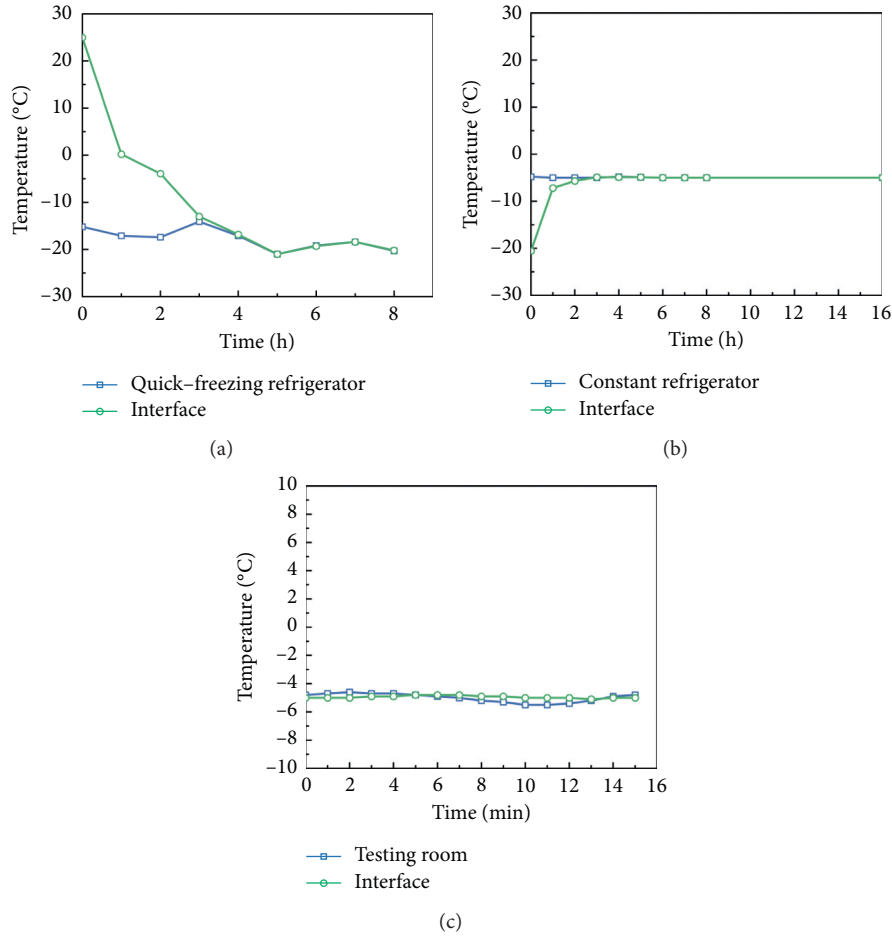


FIGURE 2: Temperature variations during quick-freezing (a), constant temperature process (b), and shearing test (c).

while it increased slightly with increasing initial water content at -5°C (Figure 4(d)). The peak shear stress varied from 126.8 kPa to 141.2 kPa with increasing initial water content at -3°C , while it increased significantly from 113.1 kPa to 399.5 kPa with the initial water content increasing from 9.2% to 20.8% at -5°C . This is because the ice content increased dramatically with the decreasing temperature and the increasing initial water content [13].

Table 2 shows the interface shear strength parameters including interface cohesion and friction coefficient at different temperatures and initial water contents. The interface cohesion presented a similar variation trend with the peak shear stress, while the effect of test temperature and initial water content on interface friction coefficient was quite small, consistent with the results in Wen et al. [13].

3. Modeling of Interface Behavior

3.1. The Nonlinear Model. The stress-displacement response of geomaterials is usually presented as strain-hardening behavior or strain-softening behavior. There are several models that can describe these behaviors, including the Duncan-Chang Hyperbolic Model, which successfully describes strain-hardening behavior [29], and the Humped

Yield Model that describes strain-softening behavior [32]. However, the strain-hardening and strain-softening behaviors often appeared simultaneously in a series of experiments. Hence, Wang et al. [42] establish a new model that could simulate the strain-hardening and strain-softening behaviors simultaneously. The model is based on a combination of the power function and the exponential function, which can be expressed by the following equation:

$$\tau = f(\delta) = [(a\delta^m - c)e^{-b\delta^n} + c]p_0, \quad (1)$$

where τ = shear stress; δ = horizontal displacement; p_0 = the standard atmosphere (101.3 kPa); e = the Euler's number; and a , b , c , m , and n are parameters. The model has the following characteristics:

- (1) $\lim_{\delta \rightarrow 0} [(a\delta^m - c)e^{-b\delta^n} + c]p_0 = 0$, the function passing through the origin
- (2) $\lim_{\delta \rightarrow \infty} [(a\delta^m - c)e^{-b\delta^n} + c]p_0 \rightarrow cp_0$, the function is bounded

These characteristics ensure that the model can simulate the stress-displacement behavior of geomaterials.

The shear stress versus horizontal displacement with different parameters of the model is shown in Figure 5. It is

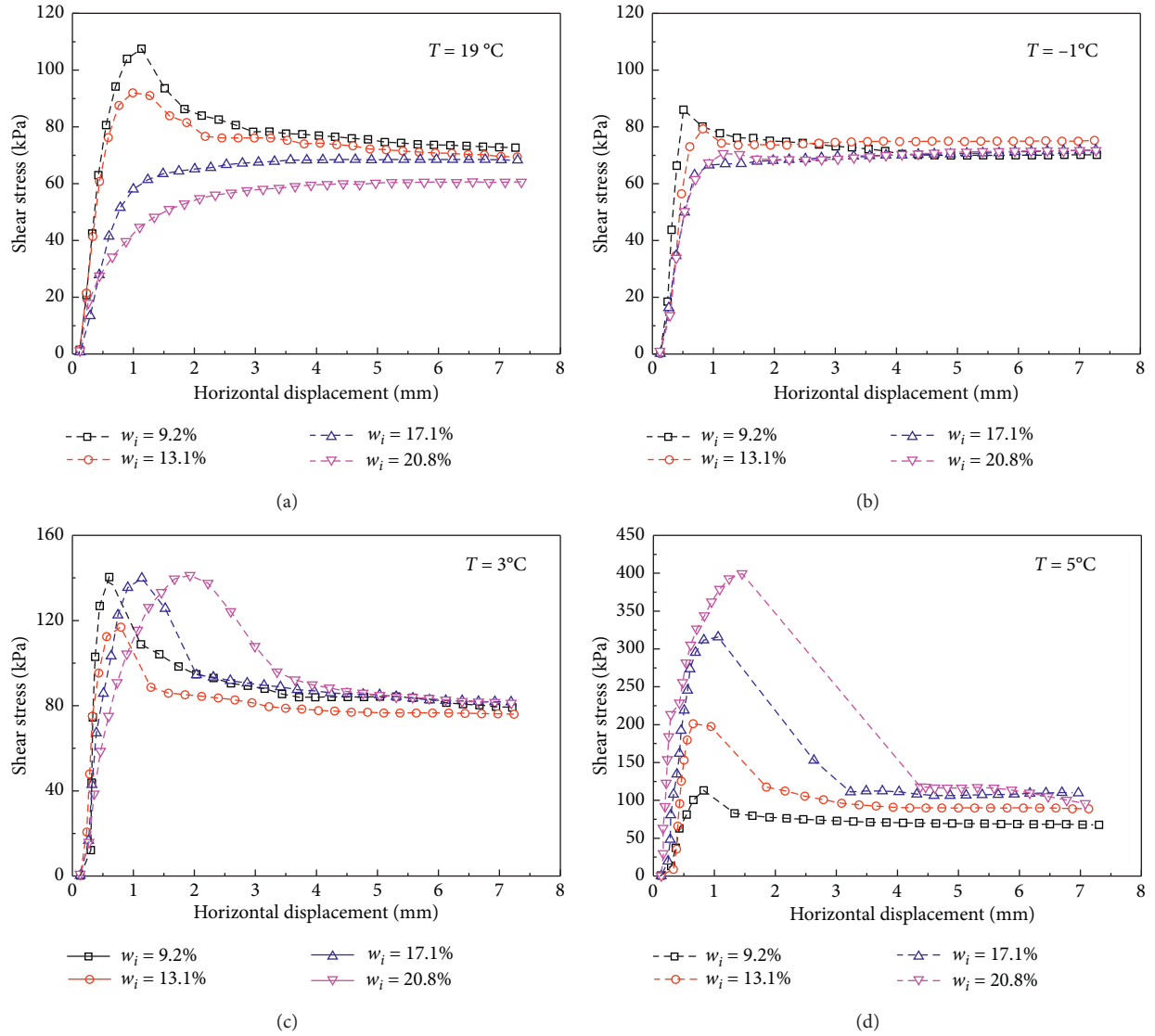


FIGURE 3: Shear stress versus horizontal displacement at the normal stress of 100 kPa. (a) ($T = 19^\circ\text{C}$), (b) ($T = -1^\circ\text{C}$), (c) ($T = -3^\circ\text{C}$), and (d) ($T = -5^\circ\text{C}$).

observed that the model can simulate behaviors including strain-softening and strain-hardening through different parameters.

3.2. Determination of the Model Parameters. There are five parameters in the model that need to be determined, which are a , b , c , m , and n , respectively. It is noted that, for the strain-softening behavior, the prepeak region is determined by the part of the exponential function ($a\delta^m$) and the postpeak region is determined by the part of power function ($e^{-b\delta^n}$) [42]. For the strain-hardening behavior, a cutoff point at 2.5% shear strain is collected to divide the nominal prepeak region and the nominal postpeak region [42]. The details are as follows:

3.2.1. Parameter c . $f(\delta) \rightarrow cp_0$ as $\delta \rightarrow +\infty$, then $c = \tau_r/p_0$, where τ_r is the residual strength for the strain-softening

behavior. At the strain-hardening behavior, $c = \tau_u/p_0$, where τ_u is the ultimate strength.

3.2.2. Parameters a and m . As mentioned above, the pre-peak region is calculated by the part of the exponential function:

$$\frac{\tau}{p_0} = a\delta^m. \quad (2)$$

Take the logarithm of the two sides of the above equation:

$$\ln\left(\frac{\tau}{p_0}\right) = \ln(a) + m \ln(\delta). \quad (3)$$

Equation (3) is a linear equation, where $\ln(\tau/p_0)$ and $\ln(\delta)$ are the variables, and $\ln(a)$ and m are the coefficients, as

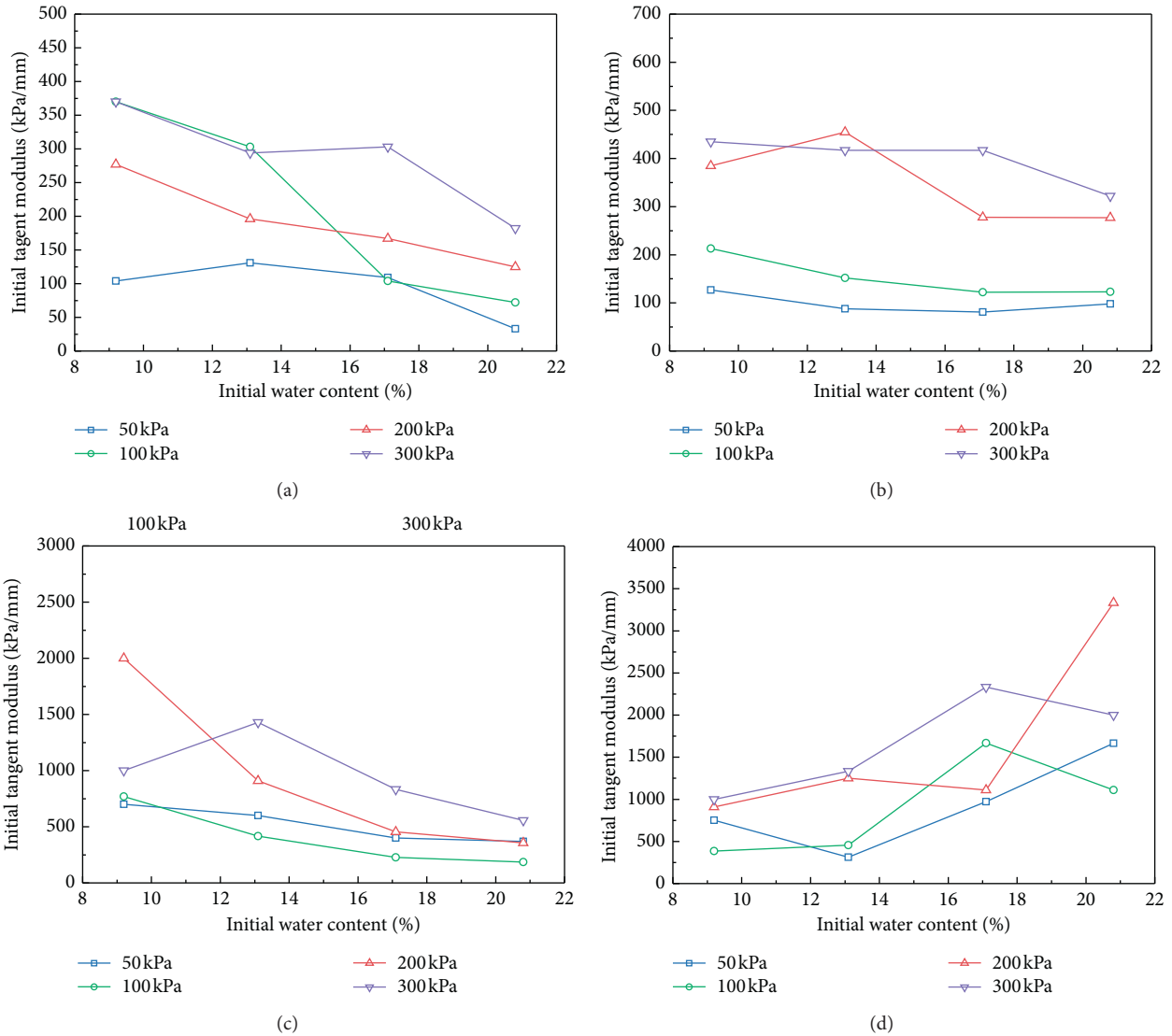


FIGURE 4: Relationship of the initial tangent stiffness with different water contents and normal stresses at a temperature of 19°C (a), -1°C (b), -3°C (c), and -5°C (d).

TABLE 2: Interface shear strength parameters.

Temperature (°C)	Initial water content (%)	Interface cohesion (kPa)	Interface friction coefficient
19	9.2	41.5	0.50
	13.1	34.8	0.53
	17.1	17.6	0.57
	20.8	3.6	0.58
-1	9.2	30.2	0.58
	13.1	26.6	0.52
	17.1	24.1	0.51
	20.8	19.3	0.52
-3	9.2	72.4	0.56
	13.1	54.1	0.63
	17.1	89.1	0.53
	20.8	79.3	0.51
-5	9.2	54.8	0.51
	13.1	145.2	0.50
	17.1	227.9	0.53
	20.8	357.7	0.40

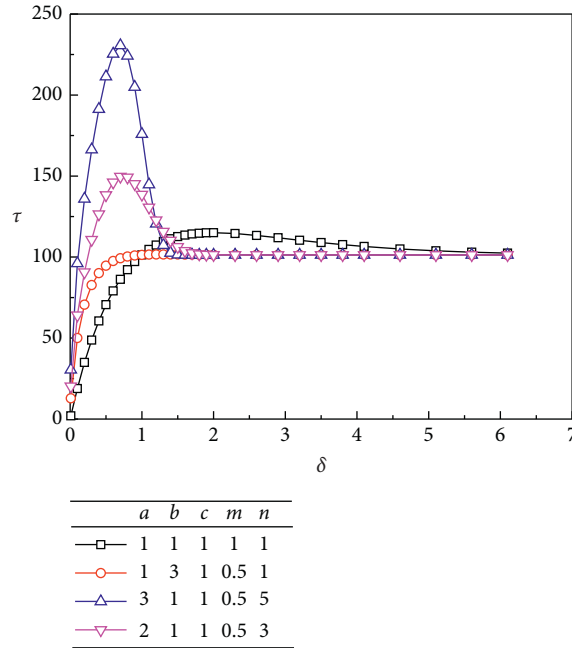


FIGURE 5: The shear stress versus horizontal displacement with different parameters.

is shown in Figure 6. The parameters *a* and *m* can be calculated by linear fitting the test results in the prepeak region.

3.2.3. *Parameters b and n.* From equation (1), equation (4) can be obtained:

$$\ln\left(\frac{a\delta^m - c}{(\tau/p_0) - c}\right) = b\delta^n \quad (4)$$

Let $\tau^* = (a\delta^m - c)/((\tau/p_0) - c)$, and then take the logarithm of the two sides of equation (4), as follows:

$$\ln(\tau^*) = \ln(b) + n \ln(\delta) \quad (5)$$

The parameters *b* and *n* can be obtained through fitting the test results in the postpeak region by equation (5), as is exhibited in Figure 7.

The parameters of the model in equation (1) can be calculated by the above method, while a more convenient method is required to calculate the parameters through the MATLAB programming function.

3.3. *Tangent Modulus.* The tangent modulus is useful in describing the behavior of geomaterials that are beyond the elastic region. They can be obtained from equation (1), which is as follows:

$$G_t = \frac{d\tau}{d\delta} = (amd^{m-1} + bcn\delta^{n-1} - abn\delta^{m+n-1})e^{-b\delta^n} p_a \quad (6)$$

The initial tangent modulus can be obtained by fitting the test results in the linear elastic region.

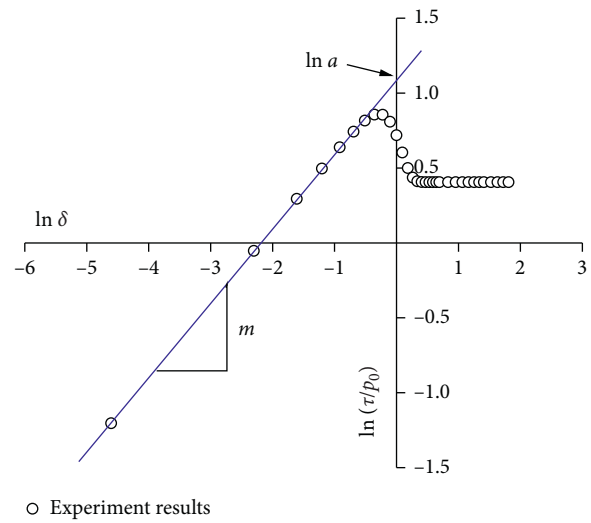
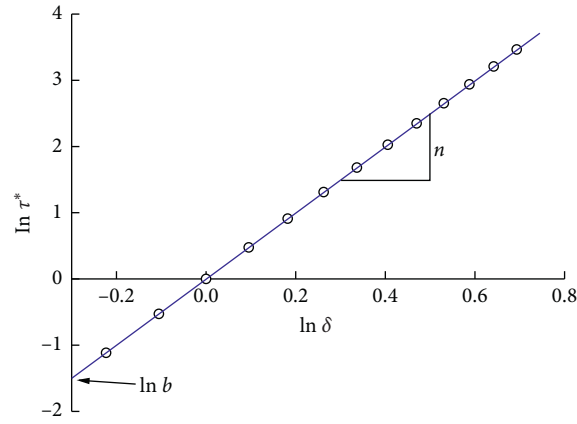


FIGURE 6: $\ln(\tau/p_0)$ versus $\ln \delta$.

3.4. *Back-Prediction and Comparison with Test Results.*

The shear stress versus horizontal displacement curves for concrete-frozen soil interfaces are shown in Figure 3. The model parameters that were calculated using the procedure as described in Section 3.2 are given in Table 3. Using the model parameters, complete shear stress horizontal displacement relationship was predicted for different temperatures and initial water contents. The experimental values and fitted curves (using equation (1)) are shown in Figure 8. Good fits were obtained for the concrete-frozen soil interface, as indicated by their coefficient of determination value (R^2) (Figure 8). It is also observed that the back-fitted curves showed a good agreement with the experimental date, both for the strain-hardening and strain-softening behaviors.

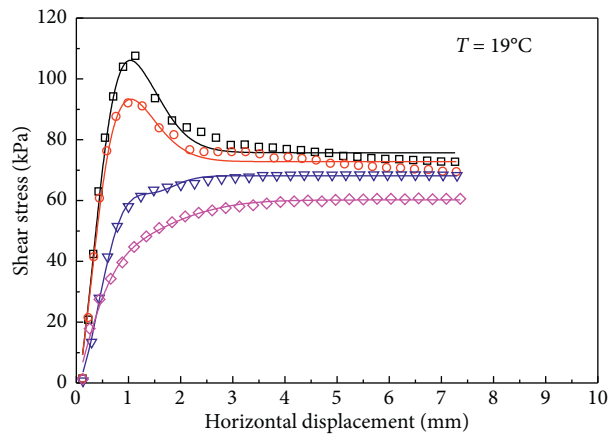


○ Experiment results at postpeak region

FIGURE 7: $\ln \tau^*$ versus $\ln \delta$.

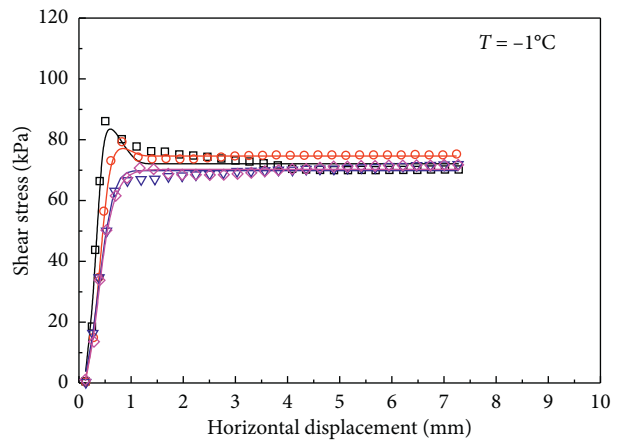
TABLE 3: Model parameters.

Temperature (°C)	Initial water content (%)	Parameters				
		<i>a</i>	<i>b</i>	<i>c</i>	<i>m</i>	<i>n</i>
19	9.2	2.57	1.75	0.75	1.97	1.49
	13.1	2.09	1.85	0.72	1.89	1.47
	17.1	-0.16	2.24	0.67	8.52	1.81
	20.8	-0.24	1.61	0.59	3.25	1.24
-1	9.2	11.40	7.25	0.71	3.26	2.62
	13.1	3.80	6.20	0.74	3.34	2.90
	17.1	0.00	5.52	0.69	2.28	2.29
	20.8	-31.49	7.95	0.69	1.68	1.06
-3	9.2	15.33	3.68	0.85	3.07	2.10
	13.1	10.02	4.03	0.78	2.65	1.98
	17.1	3.35	1.52	0.84	2.15	1.61
	20.8	1.42	0.65	0.81	1.51	1.45
-5	9.2	5.25	2.50	0.70	2.92	2.11
	13.1	28.24	3.63	0.93	4.14	2.77
	17.1	19.03	2.18	1.10	2.72	1.77
	20.8	7.93	0.91	0.99	1.25	1.29



Initial content	Experiment result	Predicted result	R^2
$w = 9.2\%$	□	—	0.9785
$w = 13.1\%$	○	—	0.9773
$w = 17.1\%$	▽	—	0.9975
$w = 20.8\%$	◇	—	0.9922

(a)



Initial content	Experiment result	Predicted result	R^2
$w = 9.2\%$	□	—	0.9770
$w = 13.1\%$	○	—	0.9983
$w = 17.1\%$	▽	—	0.9916
$w = 20.8\%$	◇	—	0.9951

(b)

FIGURE 8: Continued.

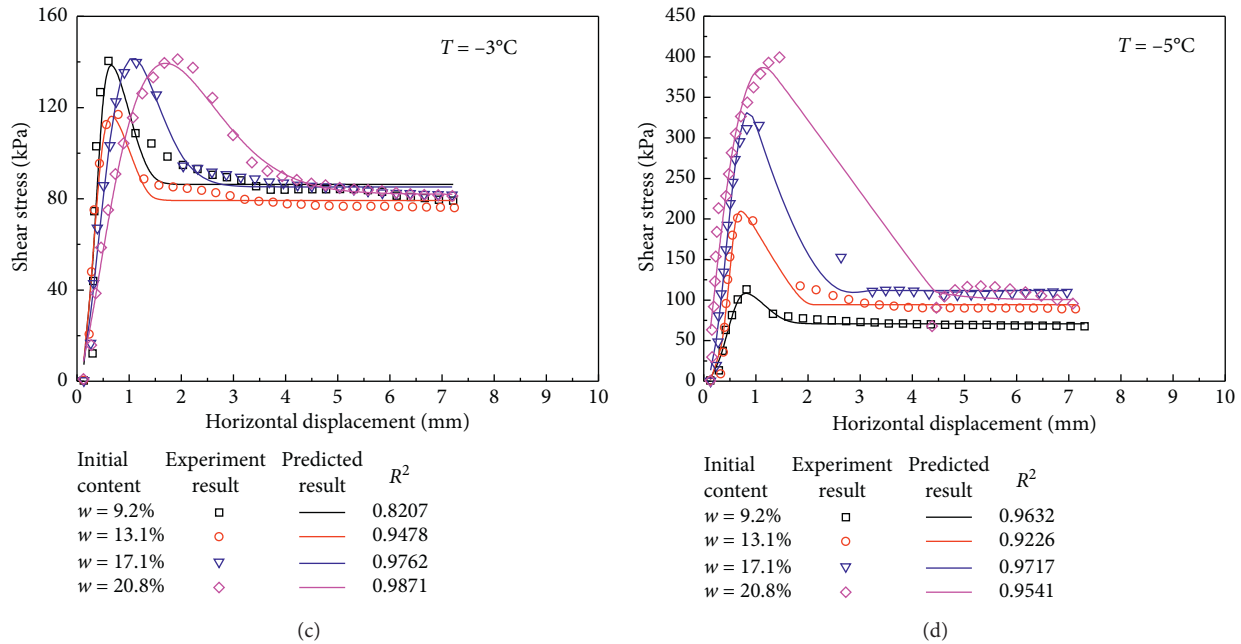


FIGURE 8: Experimental and predicted interface behaviors.

4. Conclusions

In this paper, a series of direct shear tests were carried out to determine the concrete-soil interface behaviors at different temperatures (19°C, -1°C, -3°C, and -5°C) and initial water contents (9.2%, 13.1%, 17.1%, and 20.8%). The interface shear behaviors, including shear stress versus horizontal displacement, the interface cohesion, and friction coefficient were analyzed based on the test results. A simple, nonlinear model was proposed and verified. By using the test results, the model parameters were obtained, and then the back-predictions were carried out to verify the model. The following conclusions can be drawn:

- (1) The concrete-soil interface exhibited a strain-hardening behavior at a temperature of 19°C with an initial water content of 17.1% and 20.8%, and at a temperature of -1°C with an initial water content of 20.8%. While, a strain-softening behavior was exhibited at the rest test conditions.
- (2) The interface cohesion is sensitive to the temperature and initial water content, while the interface friction coefficient is insensitive to both the factors.
- (3) The parameters of the simple model can be obtained by back-analyzing the test results. With these parameters, the back-fitted curves showed a good agreement with the experiment results both for the strain-softening and strain-hardening behaviors of the interface.

It is important to point out that the relationship of shear stress and horizontal displacement of the concrete-soil interface depends upon the specific properties of materials and experimental conditions. The model can only be used for the interfaces that show similar behaviors and responses. The

test results presented in this study can provide important data support for theoretical study on the shear behaviors of concrete-frozen soil interface.

Data Availability

The data used to support the findings of this study are included within the article.

Conflicts of Interest

The authors declare that they have no conflicts of interest.

Acknowledgments

This work was supported by the Scientific Instrument Developing Project of the Chinese Academy of Science (No. 28Y928581) and the National Natural Science Foundation of China (No. 42001058).

References

- [1] V. R. Parameswaran, "Adfreeze strength of frozen sand to model piles," *Canadian Geotechnical Journal*, vol. 15, no. 4, pp. 494–500, 1978.
- [2] N. A. Tsytoich, Y. A. Kronik, A. N. Gavrilov et al., "Mechanical properties of frozen coarse-grained soils," *Development of Geotechnical Engineering*, vol. 18, no. 4, pp. 47–53, 1981.
- [3] A. A. Aldaeef and M. T. Rayhani, *Adfreeze Strength and Creep Behavior of Pile Foundations in Warming Permafrost* "International Congress and Exhibition" Sustainable Civil Infrastructures: Innovative Infrastructure Geotechnolgy, pp. 254–264, Springer, Berlin, Germany, 2017.
- [4] X. B. Chen, J. K. Liu, H. X. Liu et al., *Frost Action of Soil and Foundation Engineering*, Science Press, China Beijing, 2006.

- [5] W. Ma and D. Y. Wang, *Mechanics of Frozen Soil*, Science Press, China Beijing, 2014.
- [6] O. B. Andersland and M. R. M. Alwahhab, "Bond and slip of steel bars in frozen sand," in *Proceedings of the CRREL Proc. Of the 3d International Symposium on Ground Freezing*, pp. 27–34, Hanover, NH, USA, April 1982.
- [7] V. R. Parameswaran, "Creep of model piles in frozen soil," *Canadian Geotechnical Journal*, vol. 16, no. 1, pp. 69–77, 1979.
- [8] E. Penner and W. W. Irwin, "Adfreezing of leda clay to anchored footing columns," *Canadian Geotechnical Journal*, vol. 6, no. 3, pp. 327–337, 1969.
- [9] G. H. Johnston and B. Ladanyi, "Field tests of grouted rod anchors in permafrost," *Canadian Geotechnical Journal*, vol. 9, no. 2, pp. 176–194, 1972.
- [10] K. W. Biggar and D. C. Segoo, "Field pile load tests in saline permafrost. i. test procedures and results," *Canadian Geotechnical Journal*, vol. 30, no. 1, pp. 34–45, 1993.
- [11] K. W. Biggar and D. C. Segoo, "Field pile load tests in saline permafrost. II. Analysis of results," *Canadian Geotechnical Journal*, vol. 30, no. 1, pp. 46–59, 1993.
- [12] Q. Feng, B. S. Jiang, Q. Zhang et al., "Reliability research on the 5cm-thick insulation layer used in the Yuximolegai tunnel based on a physical model test," *Cold Region Science and Technology*, vol. 124, pp. 54–66, 2016.
- [13] Z. Wen, Q. Yu, W. Ma et al., "Experimental investigation on the effect of fiberglass reinforced plastic cover on adfreeze bond strength," *Cold Regions Science and Technology*, vol. 131, pp. 108–115, 2016.
- [14] J. Liu, P. Lv, Y. Cui, and J. Liu, "Experimental study on direct shear behavior of frozen soil-concrete interface," *Cold Regions Science and Technology*, vol. 104-105, pp. 1–6, 2014.
- [15] L. Z. Zhao, P. Yang, L. C. Zhang et al., "Cyclic direct shear behaviors of an artificial frozen soil-structure interface under constant normal stress and sub-zero temperature," *Cold Region Science and Technology*, vol. 133, pp. 70–81, 2017.
- [16] Q. B. Shi, P. Yang, and G. L. Wang, "Experimental research on adfreezing strengths at the interface between frozen fine sand and structures," *Science of Iranica Transaction A, Civil Engineering*, vol. 25, no. 2, pp. 663–674, 2018.
- [17] T.-L. Wang, H.-H. Wang, T.-F. Hu, and H.-F. Song, "Experimental study on the mechanical properties of soil-structure interface under frozen conditions using an improved roughness algorithm," *Cold Regions Science and Technology*, vol. 158, pp. 62–68, 2019.
- [18] C. S. Desai and E. C. Drumm, "Interface model for dynamic soil-structure interaction," *Journal of Geotechnical Engineering*, vol. 110, no. 9, pp. 1257–1273, 1984.
- [19] A. Foriero and B. Ladanyi, "FEM simulation of interface problem for laterally loaded piles in permafrost," *Cold Regions Science and Technology*, vol. 23, no. 2, pp. 121–136, 1995.
- [20] H. Liu and H. I. Ling, "Constitutive description of interface behavior including cyclic loading and particle breakage within the framework of critical state soil mechanics," *International Journal for Numerical and Analytical Methods in Geomechanics*, vol. 32, no. 12, pp. 1495–1514, 2008.
- [21] J. Liu, D. Zou, and X. Kong, "A three-dimensional state-dependent model of soil-structure interface for monotonic and cyclic loadings," *Computers and Geotechnics*, vol. 61, no. 61, pp. 166–177, 2014.
- [22] L. Zhao, P. Yang, J. G. Wang, and L.-C. Zhang, "Impacts of surface roughness and loading conditions on cyclic direct shear behaviors of an artificial frozen silt-structure interface," *Cold Regions Science and Technology*, vol. 106-107, pp. 183–193, 2014.
- [23] T. L. Wang, H. H. Wang, T. F. Hu et al., "Experimental study on the mechanical properties of soil-structure interface under frozen conditions using an improved roughness algorithm," *Cold Regions Science and Technology*, vol. 158, pp. 62–68, 2019.
- [24] Y. J. Ji, K. Jia, Q. H. Yu et al., "Direct shear tests of freezing strength at the interface between cast-in-situ concrete and frozen soil," *Journal of Glaciology and Geocryology*, vol. 39, no. 1, pp. 86–91, 2017.
- [25] A. V. Sadovskiy, "adfreeze between ground and foundation materials," in *Proceedings of the 2nd International Conference On Permafrost*, pp. 650–653, Yakustsk, Russia, July 1973.
- [26] J. S. Weaver and N. R. Morgenstern, "Simple shear creep tests on frozen soils," *Canada Geotechnical Journal*, vol. 18, no. 18, pp. 217–229, 1981.
- [27] P. Lv and J. K. Liu, "An experimental study on direct shear tests of frozen soil- concrete interface," *Journal of The China Railway Social*, vol. 37, no. 2, pp. 106–110, 2015.
- [28] Q. Z. Wang, X. X. Zhu, J. K. Liu et al., "Experimental study on direct shear tests of coarse-grained fillings of High-speed railway subgrade in cold region," *Journal of The China Railway Social*, vol. 38, no. 8, pp. 102–109, 2016.
- [29] J. M. Duncan and C. Y. Chang, "Nonlinear analysis of stress and strain in soils," *Journal of Soil Mechanics and Foundation Division*, vol. 96, no. 5, pp. 1629–1653, 1970.
- [30] A. N. Gitau, L. O. Gumbe, and E. K. Biamah, "Influence of soil water on stress-strain behaviour of a compacting soil in semi-arid Kenya," *Soil and Tillage Research*, vol. 89, no. 2, pp. 144–154, 2006.
- [31] J. H. Zhang, Z. H. Chen, N. Zhao et al., "A new nonlinear model of unsaturated soils and its application," *Rock and Soil Mechanics*, vol. 37, no. 3, pp. 616–624, 2016.
- [32] Z. D. Liu, J. Li, Z. Y. Guo et al., "Deformation behaviors and deformation parameter of loess in Shaanxi district," *Chinese Journal of Geotechnical Engineering*, vol. 6, no. 3, pp. 24–34, 1984.
- [33] L. Hu and J. Pu, "Testing and modeling of soil-structure interface," *Journal of Geotechnical and Geoenvironmental Engineering*, vol. 130, no. 8, pp. 851–860, 2004.
- [34] G. Zhang and J. M. Zhang, "Unified modelling of soil-structure interface and its test confirmation," *Chinese Journal of Geotechnical and Engineering*, vol. 27, no. 10, pp. 1176–1179, 2005.
- [35] D. J. Zhang and T. H. Lu, "Establishment and application of an interface model between soil and structure," *Chinese Journal of Geotechnical Engineering*, vol. 20, no. 6, pp. 62–66, 1998.
- [36] Z. Zhu, F. Xing, W. Qu et al., "Fractal description of two phase medium cementation plane roughness coefficient between rock and concrete," *Chinese Journal of Geotechnical Engineering*, vol. 31, no. 1, pp. 20–25, 2006.
- [37] C. S. Desai and Y. Z. Ma, "Modeling of joints and interfaces using the Disturbed-stated concept," *International Journal for Numerical and Analytical Methods in Geomechanics*, vol. 16, no. 1, pp. 623–653, 1992.
- [38] GB/T50123-1999, *The Standard of Chinese Soil Test Method*, National Standard of China, Taiwan, China, 1999.
- [39] GBJ-145-90, *Standard for Soil Classification*, National Standard of China, Taiwan, China, 1991.
- [40] GBJ-82-85, *The Test Method of Long Term and Durability on Ordinary Concrete*, National Standard of China, Taiwan, China, 1997.
- [41] N. Lu and W. J. Likos, *Unsaturated Soil Mechanics*, John Wiley & Sons, Inc, Hoboken, NJ, USA, 2004.

- [42] L. Q. Wang, Z. G. Lu, and S. J. Shao, "A composite power exponential nonlinear model of rock and soil," *Chinese Journal of Rock Mechanics Engineering*, vol. 39, no. 9, pp. 1724–1730, 2017.